Different modular techniques applied in a synchronous boost converter with SiC MOSFETs to obtain high efficiency at light load and low current ripple

Aitor Vazquez, *Member, IEEE*, Alberto Rodriguez, *Member, IEEE*, Maria R. Rogina, *Student Member, IEEE*, Diego G. Lamar, *Member, IEEE*.

Abstract— This paper is focused on a high voltage (400V to 800V) bidirectional converter which is intended to be used for the interconnection of battery based energy storage systems with the cells of a Modular Multilevel Converter (MMC), providing distributed energy storage capability to a Solid State Transformer (SST). This converter must have a high efficiency at medium and light load and also a low current ripple due to the charging and discharging processes. This work takes advantage of the use of SiC MOSFETs into a synchronous boost converter to accomplish the previous requirements. First, the adoption of a variable switching frequency control to keep the efficiency high is analyzed. And second, the use of a modular converter with different control techniques to provide a current ripple reduction is also addressed in this work. An Input Parallel Output Parallel (IPOP) synchronous boost converter, made up with 3 modules (3kW per module) is used to validate experimentally the advantages of the use of SiC MOSFETs and to compare different control techniques.

Index Terms— Modular converters, DC/DC bidirectional converters, light load, SiC MOSFETs.

I. INTRODUCTION

POWER Electronics Transformers (PETs), also called Solid State Transformers (SSTs), are envisioned as a semiconductor based alternative to conventional Line-Frequency Transformers (LFTs) [1]. PETs are expected to beat the LFTs in terms of power density and much superior functionalities, but would be inferior in terms of cost, efficiency (full load) and reliability [1]-[4]. A fully modular three stage approach (AC/DC + DC/DC + AC/DC) appears to be the most popular choice [2], [5]-[8]. Based on the modular approach, the use of multilevel converters to develop the AC/DC stage of the PET is very common, as in the case Cascaded H-Bridge (CHB)-based PET [8] and Multilevel Modular Converter (MMC)-based PET [9], [10]. Multilevel converters have several convenient characteristics [11]-[13], being a distinguishing one the fact that while it provides a high voltage DC link, the distributed energy storage at the cells capacitors eliminates the need of a bulk DC capacitor, which is advantageous for safety and reliability reasons [14].

In PETs based in multilevel converters, it is possible to add, by adequate design of the cells, a multiport capability, able to integrate at the cell level low voltage dc or ac power sources, loads or energy storage devices and/or systems. The inclusion of distributed energy storage capability can be carried out integrating storage systems at the cell level. However, if the voltage value at the cell and the storage system are different, the use of bidirectional power converters is mandatory to adapt the energy format.

When a bidirectional power converter is used to connect the storage system to the cell, a small part of the energy is lost in the charge and discharge process of the storage system. Consequently, a highly efficient converter must be designed. Depending on the voltage levels of the storage system and the cell, different power converters topologies can be used. To reduce the number of cells in a multilevel converter, the voltage at the cell is usually high, in the order of 1000V (in this work 800V) and high voltage storage systems are typically required (in this work 400V), mainly for this reason, non-isolated power converters can be used.

In this paper, an Input Parallel Output Parallel (IPOP) modular synchronous DC/DC boost converter is developed in order to integrate storage capability in a MMC-based PET under development. A variable switching frequency operational mode (Quasi-Square Wave Mode, QSW-ZVS) is adopted to provide high efficiency over a wide output power range, especially at light loads. This is mainly due to battery charging process, which is usually done in three stages [15], with a final stage in which the charging current is very low (i.e. low load or low output power level). Working in this QSW-ZVS operational mode, the controller has to increase the switching frequency several orders of magnitude when power decreases.

Hence, to comply with high voltage and switching frequency requirements, the use of Silicon Carbide (SiC) power MOSFETs is proposed to take advantage of their properties. As it is already known new Wide Band-Gap (WBG)

The authors are with University of Oviedo, Electronic Power Supply Systems group, Edificio 3, Campus de Viesques s/n, 33204 Gijon, SPAIN (e-mail: vazquezaitor@uniovi.es).

semiconductors, especially SiC or Gallium Nitride (GaN) transistors can withstand higher voltage levels, allowing faster switching and lower conduction losses, in comparison with similar silicon-based transistors [16]. The use of SiC power MOSFETs provides a higher attainable switching frequency, which is especially interesting in variable frequency control techniques. This capability, makes possible the use of QSW-ZVS in high voltage and high power applications providing a high efficiency at light loads (even at high switching frequency). This is one contribution of this paper.

One of the disadvantages of QSW-ZVS operational mode, is the required large inductor current ripple which is precisely unsuitable for energy storage systems. High charge current ripple levels increase the aging and derating effects among the charging and discharging processes of the battery [17]. However, this drawback can be overcome by the use of modular converters (i.e. multi-phase interleaved converters connected in parallel) in order to reduce this charge current ripple.

The combination of different operational modes and modularization techniques (to keep high efficiency at light load and low charge current ripple, respectively) are evaluated in this paper. In fact, all of them are both conceived and applied to an IPOP modular converter based on bidirectional DC/DC boost converters using SiC power MOSFETs, presenting advantages and disadvantages of each one in comparison to each other's. As it was stated before, one of the advantages of SiC power MOSFETs is the increase of the maximum attainable switching frequency. Consequently a wider power range with high efficiency can be obtained. Considering this improvement, the comparison of the performance of these techniques, making possible a certain selection criteria for specific applications, is another contribution of this paper.

This paper is organized as follows. In Section II, the requirements of the power devices that composed a MMC-based PET with integrated and distributed energy storage systems are presented, and therefore, the justification of the use of SiC MOSFETs are also stated. In Section III, the most common control techniques applied to a bidirectional boost DC/DC converter are reviewed, focusing on QSW-ZVS. Section IV shows a deep analysis of the proposed control and modularization techniques to keep high the efficiency at light load and to reduce the charge current ripple of the proposed system. Different combinations of operational modes and modularization techniques are explained and compared, emphasizing their advantages and disadvantages. In Section V, details about the design of the modular converter and the experimental results are presented. Finally, conclusions are presented in Section VI.

II. POWER DEVICES REQUIREMENTS

A potential configuration for a three-stage multiport PET is derived from the MMC topology, where an isolated and bidirectional DC/DC converter (being a Dual Active Bridge (DAB) usually preferred) is used to inject/drag power from the MMC HB cells. The low voltage (LV) side of the DABs are parallelized to form a low-voltage, high-current DC link [9], [10]. The MMC-based PET provides three ports: high-voltage DC (HVDC), high-voltage AC (HVAC) and low-voltage AC

(LVAC), being therefore a multiport power converter where all the ports are bidirectional.

It is possible, however to connect elements to the DC link of the cells [10]. These can include energy storage elements [18] or distributed energy resources (DER) [19]. This is schematically shown in Fig. 1 (non-isolated dc-dc power converter highlighted in green). In this case, some cells are connected in parallel using DABs to perform the AC/AC power conversion with galvanic isolation and other cells are connected to energy storage elements and DER using non isolated DC/DC power converters. The converter connecting the DER/energy storage to the MMC cell does not have to be necessarily a DAB, it can be optimized for the specific needs (e.g. galvanic isolation or bidirectional power flow capability).

The converter presented in this work is oriented to provide energy storage capability to a MMC-based PET. However, the conclusions obtained could be applied to different applications, where a bidirectional converter with high efficiency for light loads and high voltage operation is required (e.g. wind energy generation with storage capability [20] or Electric Vehicle (EV) battery chargers [21], [22]).

In this work, the cell voltage (V_{cell}) being considered is 800V. Therefore, two options can be considered: Si IGBTs or SiC MOSFETs. A synchronous boost converter is chosen for interfacing the battery with the cell. QSW-ZVS operational mode can be applied to this converter, in order to obtain a very high efficiency al medium and light load. In this operational mode, the switching frequency increases when power decreases. Then, the switching frequency may vary several orders of magnitude from full load to light load (from tens of kHz up to hundreds of kHz). So, the use of SiC MOSFETs allows a higher maximum switching frequency and, consequently, the range of power with high efficiency can be wider using this specific operational mode.
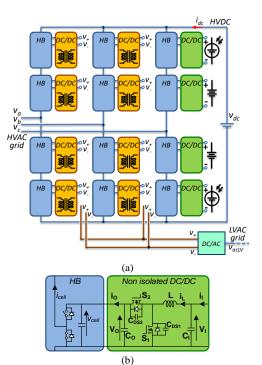

(a)

(b)

Fig. 1. (a) DER and/or energy storage integration in an MMC. (b) Example of a structure of a cell with distributed energy storage systems.

III. OPERATIONAL MODES FOR SYNCHRONOUS BOOST CONVERTER

A synchronous boost converter is the simplest bidirectional topology without galvanic isolation (Fig. 2). The low number of components needed and the large number of different control techniques (providing different operational modes) which can be applied to this topology are its main advantages. A possible way to obtain very high efficiency is to use QSW-ZVS. This operational mode can be applied to traditional DC/DC topologies (buck, boost and buck-boost converter families) for reducing the switching losses [23]-[30]. In a boost converter, to properly work in QSW-ZVS, the output voltage should be higher than twice the input voltage [25] and [27]. Furthermore, the inductance value should be low, hence, the converter works with a large inductor current ripple. The theoretical inductor current waveform of a synchronous boost converter working in QSW-ZVS mode can be seen in Fig. 3(a).

In this converter there are two different dead times. The first dead time (t_{d1}) is constant and it is located after the magnetizing interval (i.e. after $S1$ turns-off, before $S2$ turns-on). The lowest limit for the first dead time (t_{d1}) is constrained by the need to avoid a short-circuit when $S2$ is turned on and $S1$ is turned off. On the other hand, excessive large values of t_{d1} will result in increased losses introduced by the conduction of the parasitic body diode of $S2$. This first dead time is usually omitted in the analysis of this operational mode.

The second dead time (t_{d2}) is placed after the demagnetizing interval (i.e. before $S1$ turns-on, after $S2$ turns-off. During this second dead time the inductance current becomes negative and a resonance with the parasitic output capacitance of the transistors occurs. Based on this resonance, S_1 output capacitor might be fully discharged during t_{d2} (i.e. S_1 turn-on) and then Zero Voltage Switching (ZVS) condition can be achieved. Moreover, it should be noted that S_2 is turned-off under Zero Current Switching (ZCS). Hence, the switching losses are drastically reduced. In order to keep constant the reactive current needed to achieve ZVS, the switching frequency must
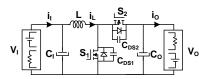

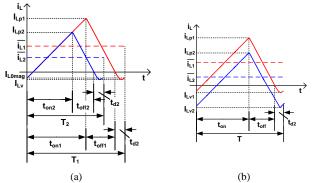Fig. 2. Synchronous boost converter.

(a)   (b)

Fig. 3. Inductor current waveform at full load and at medium load for a synchronous boost converter. (a) Working in QSW-ZVS mode. (b) Working in TCM mode. The first dead time (t_{d1}) has been omitted.

be increased when the output power decreases. In this mode, the maximum switching frequency of the power devices f_{smax} determines the minimum power. This minimum power can be calculated as

$$P_{min} = V_I^2 \cdot \frac{D}{2L} \cdot \frac{1}{f_{smax}} \qquad (1)$$

Thanks to the low parasitic capacitances of SiC MOSFETs, f_{smax} can be greatly increased, allowing the use of QSW-ZVS for very light loads.

Another possibility is to use Triangular Current Mode (TCM) which is another operational mode very similar to QSW-ZVS. The main difference between these operational modes is that TCM works at constant switching frequency increasing the reactive current at light load and keeping inductor current ripple constant (see Fig. 3(b)). TCM mode is more suitable for narrow load variations, because at light load condition conduction losses are increased drastically due to the large amount of reactive current.

IV. MODULAR TECHNIQUES FOR IPOP BOOST CONVERTER

In spite of TCM and QSW-ZVS modes have the great advantage of reducing switching losses, both modes have the disadvantage of working with a large inductor current ripple as can be seen in Fig. 3. For energy storage system applications, such as battery chargers or supercapacitors, this large charge current ripple may either reduce the life span of the energy storage system or derate its functionalities. Based on this, a possible way to overcome this problem is to use some modular approach in which several synchronous boost converters can be connected in parallel, and therefore, an interleaving approach can be applied in order to reduce the inductor current ripple.

Moreover, the modular approach can also be used to increase the power managed by the system. At this point, an IPOP modular converter, in which all the modules share the input and output voltage and the total input and output currents are the sum of the current of each single module, is suitable to overcome high current ripple if an interleaving control technique is applied to TCM or QSW-ZVS. In Fig. 4, a generic scheme of an IPOP modular converter is shown. The efficiency of this IPOP modular converter can be expressed as

$$\eta_T = \frac{P_O}{P_I} = \frac{V_O \cdot I_O}{V_I \cdot I_I} = \frac{V_O \cdot \sum_{n=1}^{N} I_{On}}{V_I \cdot \sum_{n=1}^{N} I_{In}} = \frac{\sum_{n=1}^{N} P_{On}}{\sum_{n=1}^{N} P_{In}} \qquad (2)$$

where P_{on} and P_{in} are the output and input voltages of a given module (module n), P_I and P_O the input and output power of the modular converter, I_{in} and I_{on} the input and output current of each module and N the number of modules. Equation (2) can be rewritten in terms of losses as

$$\eta_T = \frac{P_O}{P_I} = \frac{P_I - P_{LT}}{P_I} = \frac{P_I - \sum_{n=1}^{N} P_{Ln}}{P_I} \qquad (3)$$

where P_{Ln} are the power losses of the module n and P_{LT} the power losses of the modular converter.

These expressions are valid in an IPOP modular converter independently of the control technique implemented for its control. Hence, the overall converter efficiency can be improved, especially at medium and light load by using a properly control technique regarding the sequence of turn-of and turn-on of each module that performs the modular converter.
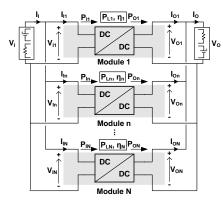
Fig. 4. Generic scheme of an IPOP modular converter.

A. Balanced technique. Master-slave approach.

A balanced technique is performed when all the modules always provide the same amount of output power (i.e. they are power balanced at any load level). So, the overall efficiency of the modular converter can be calculated using (2) and (3)

$$\eta_T = \frac{P_O}{P_I} = \frac{V_O \cdot \sum_{n=1}^{N} I_{On}}{V_I \cdot \sum_{n=1}^{N} I_{In}} = \frac{V_O \cdot N \cdot I_{On}}{V_I \cdot N \cdot I_{In}} = \eta_n \qquad (4)$$

$$\eta_T = \frac{P_I - P_{LT}}{P_I} = \frac{P_I - N \cdot P_{Ln}}{P_I} \qquad (5)$$

As can be seen in (4), the overall efficiency is exactly the efficiency of one module. Therefore, this technique does not take any advantage of the modular arrangement in terms of loss reduction at light load. However, the main advantage of this balanced technique is the input port current ripple reduction thanks to the interleaving control technique. It is very well known the relationship between the input current ripple as a function of the duty cycle (D) and the number of modules [31]. Depending on the value of D, the total input port current ripple may even be fully cancelled.

A master-slave approach can be considered to implement this balanced technique [32]. In this case, the variable controls of all the modules are the same, and they are generated and shared by the master module with the slave modules.

TCM operational mode is the simplest solution to minimize the input port current ripple. However, from the efficiency point of view, this technique is not given any advantage from the modular design, neither from the use of SiC power MOSFETs at light load. This is because, as was stated previously, TCM has a poor efficiency due to the reactive current which has to be managed.

The complexity of the master module in QSW-ZVS is slightly higher than in TCM, because this module has to generate more variable controls (switching frequency changes with the power level). All the modules work varying their switching frequency following master module variation, making also possible the interleaved technique. The main disadvantage of this technique is that the current sharing depends on the component tolerances and the differences among the modules, as in the previous case. As was previously stated, the efficiency of the modular converter is equivalent as the efficiency of one module. In QSW-ZVS, thanks to the use of SiC power MOSFETs, the efficiency of one module (and, consequently, the efficiency of the modular converter) is kept high in a wide power range (from 100% to roughly 10%, as it will be shown in Section V).

As conclusion, balanced control technique using either QSW-ZVS or TCM operational mode reduces the input current ripple. This technique is a very simple way to extend to higher power converters the high efficiency at light load thanks to the use of SiC power MOSFETs and QSW-ZVS.

B. Phase-shedding technique

The phase-shedding technique is another possible approach to control IPOP modular converters. Under this approach, only the number of modules needed to provide the total output power are working at the same time, being off if they are not used. Hence, when the output power increases, the number of active modules increases and vice versa. Therefore, the overall modular converter efficiency can be improved at medium and light load conditions [33]. However, the input current ripple reduction is worse than the obtained one for balanced technique. This is because the number of active modules changes with the load, and, therefore, the phase-shift among them in order to perform interleaving changes too, causing that the input port current ripple reduction will not be the optimum one. This drawback arises especially at light load condition, when only a few number of modules (a couple or even just one of them) are active.

A power profile example of phase-shedding technique using TCM is given in Fig. 5(a). When the total power demanded by the load is lower than P_T/N only the master module is active. When power increases higher than P_T/N, then a slave module is activated adapting its output power to the load demand. This behavior is repeated when power increases every multiple of P_T/N. When power decreases, the process is obviously reversed. In this case, efficiency at light load is improved thanks to the phase-shedding technique. This improvement is not carried out by the use of SiC power MOSFETs. However, the results obtained with this technique when operating in TCM may be used as a reference for QSW-ZVS in order to compare them.

Using QSW-ZVS, the phase-shedding technique is even more complex to be applied, once again, due to the variable switching frequency control. A possible way to adopt the phase-
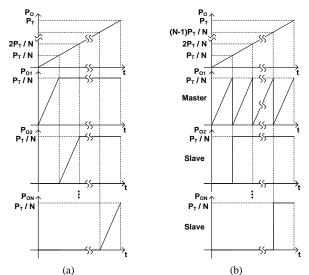

Fig. 5. Power profile example for phase-shedding technique. (a) For TCM mode. (b) For QSW-ZVS mode.

shedding technique for an IPOP QSW-ZVS modular converter was developed for a master-slave approach in [32]. However, here the master module is the only which operates in closed loop, whilst the slave modules work in open loop. The master is the only module with the capability to change its power, because the slave modules can only work in two stages: providing its maximum power (i.e. being active) or being disconnected. A power profile example of phase-shedding technique using QSW-ZVS is given in Fig. 5(b). When the total power demanded by the load is lower than P_T/N only the master module is active. When power increases higher than P_T/N, then a slave module is activated and the master module reduces its output power to provide exactly the total output power demanded by the load. This behavior is repeated every multiple of P_T/N. When power decreases, this process is reversed and the slave modules are disconnected sequentially to adjust the total power demanded by the load.

The main advantage of this technique is its simplicity. Only a slave manager is needed to develop this control, and it is easy to be implemented in a digital platform. This slave manager controls the number of active slaves operating at maximum output power. This fact, allow the slave manager to adjust the phase-shift among the slave modules for reducing the input port current ripple.

Under this technique, the slave modules can be easily interleaved due to the constant switching frequency operation (i.e. they do not vary their power). The master module has to vary its switching frequency according to QSW-ZVS operation to provide exactly the amount of power demanded by the load. Consequently, it is not possible to apply the classic interleaved (i.e. adding a certain phase-shift at modules that operates at the same switching frequency). This disadvantage has an important consequence in the IPOP modular converter performance, which is that not only the input port current ripple reduction is worse than the balanced technique but it is also worse than the TCM phase-shedding technique, especially at light load condition, when few slave modules are working together.

The application of the phase-shedding technique to QSW-ZVS allows to slightly increase the overall efficiency of the IPOP modular converter, because the slave modules work at full power and at constant frequency, which is an advantage over the balanced technique in terms of losses. Phase-shedding technique extends to a wider power range (from 100% to roughly 5%, as it will be shown in Section V) the high efficiency at light load obtained thanks to the use of SiC power MOSFETs and QSW-ZVS.

Taking into consideration the aforementioned explanations, the overall modular converter power losses applying phase-shedding technique (P_{LT_ps}) can be calculated as

$$P_{LT-ps} = P_{Ln-ps} + n_{ps} \cdot P_{Ln-ps@Pmax} \qquad (6)$$

where P_{Ln-ps} are the power losses of the module which is varying its output power, $P_{Ln-ps@Pmax}$ are the power losses of an active module which is processing its maximum output power and n_{ps} is the number of active modules processing its maximum output power (n_{ps} might vary from 0 up to N-1). It should be highlighted that (6) is also valid for the master-slave with phase-shedding approach, in which P_{Ln-ps} will be the total power losses of the master module and $P_{Ln-ps@Pmax}$ will be the

total power losses of a slave and n_{ps} will be the number of active slaves.

C. Qualitative comparison.

Based on the aforementioned characteristics of each operational mode and control technique, a brief qualitative comparison of the four combinations is done in this section. This comparison is established based on five key design parameters of the IPOP modular converter taking into account possible applications (e.g. DER and/or energy storage integration in an MMC): the input port current ripple, power losses from medium to full load, power losses from light to medium load, complexity of the control stage and switching frequency variation (or the electromagnetic emissions, EMI). For a fair comparison, the same number of modules are taken for both techniques (i.e. balanced and phase-shedding). Also, the same inductance value, transistors and capacitors are kept for all the modules and for both operational modes (TCM and QSW-ZVS). The results are summarized in Fig. 6.

These results are carried out in a qualitative way, and they can only be used for comparing the control techniques. The input current ripple is established taking into account if the interleaved approach is possible with all the modules or not. Following this criteria, a high value of this parameter is set if the input current ripple depends on the power or switching frequency, as in the case of QSW-ZVS with phase-shedding. The power losses at medium load and light load are set as low based on two considerations. First, if the control keeps the converter working with the minimum amount of reactive current. And second, if the modular control technique keeps the converter working with the minimum number of modules. The control complexity parameter strongly depends on how both operational modes and both control techniques will be implemented. Obviously, the quantification of this parameter is very subjective. In this case, the number of closed loop modules, the phase-shift to be applied among the modules and the variable switching frequency operation are considered to evaluate this parameter. Finally, the switching frequency variation depends not only on the operational mode, but also on the control technique. For instance, QSW-ZVS with phase-shedding has lower frequency variation than QSW-ZVS balanced, thanks to the open loop operation of the slave modules (i.e. in the former, all the modules vary their frequency, in the latter only one module).
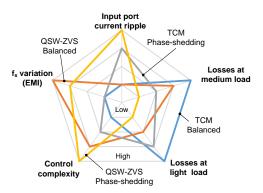

Fig. 6. Qualitative comparison for several parameters among the four options (both operational modes and both IPOP control techniques).

As can be seen, to select an appropriate control technique and operational mode, a trade-off among these parameters might be established, depending on the final application. As an example, if the input port current ripple is critical, then QSW-ZVS with balanced technique is the most suitable approach, being QSW-ZVS with phase-shedding the worst. On the other hand, if the efficiency at very light load is more relevant for the final application, then this QSW-ZVS with phase-shedding becomes the most suitable approach.

V. EXPERIMENTAL RESULTS

A. Experimental setup

For testing and comparing the four different approaches, a 3 module IPOP modular converter based on synchronous DC/DC boost converter has been built in the laboratory. The total output power is set up to 9kW (3kW per module). Input and output voltages are chosen as 400V and 800V respectively. Hence, as power transistor, the SiC MOSFET module CCS050M12CM2 (three half-bridge, six pack module) by Wolfspeed is chosen. It is important to note that each half bridge of the six pack module is used here to perform the switches of each module of the IPOP converter. The commercial driver used is CGD15FB45P1, also by Wolfspeed. The control stage has been implemented using a Spartan 3 FPGA and the control signals are sent to the driver using optic fibers. A schematic and a picture of the prototype are shown in Fig. 7. The switching frequency at full load is set to 20kHz for minimizing the switching losses and avoiding the audible noise. This switching frequency is increased in QSW-ZVS when output power is reduced. As it obvious, the switching frequency cannot be increased indefinitely in this mode for practical reasons. So, the maximum switching frequency is limited to 200kHz in this prototype. The inductors are constructed using Litz wire and an ETD59-3F3 ferrite core. All these parameters are summarized in TABLE I.

The efficiency in all the cases was measured once the converter temperature is stabilized. Heatsink with natural convection was used to dissipate the heat of the SiC MOSFETs. Input and output voltages and currents were measured using four calibrated digital multimeters (FLUKE 187). The calculated efficiencies are intended mainly for comparison purpose because the prototype has not been huge optimized. Moderate optimization have been carried out in the design of modules, and as a consequence, the efficiencies values obtained are high. At this point, it is important to note that the efficiency for all modes of operation might be slightly improved, however, the conclusion of the comparison will be the same. As a first approach, the theoretical and measured efficiency for one module of the IPOP converter are plotted in Fig. 8 for QSW-ZVS and TCM operational modes. As can be seen, both operational modes obtained roughly the same efficiency from medium to full load. However, below medium load, the efficiency of TCM is lower than the efficiency of QSW-ZVS, as it was expected.

In Fig. 9, some experimental waveforms of a single module of the IPOP converter are shown. Particularly, in Fig. 9(a) the waveforms obtained at full load are depicted. It should be noted that for both QSW-ZVS and TCM modes working at full load, these waveforms are the same. The same waveforms at light load condition are shown in Fig. 9(b) and Fig. 9(c) for TCM and
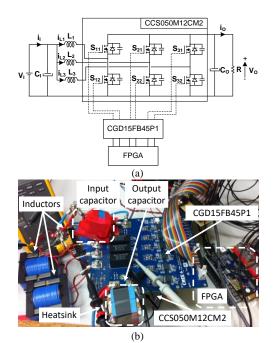

(a)

(b)

Fig. 7. Experimental prototype. (a) Schematic of the experimental setup. (b) Picture of the prototype.

TABLE I.
MAIN SPECIFICATIONS OF THE IPOP MODULAR BOOST CONVERTER.

Parameter	Value
V_I	400V
V_O	800V
P_{MAX}	9kW (3kW per module)
f_s	20kHz (at full load)
L	600µH per module
MOSFET	CCS050M12CM2 1200V, 50A, 25mΩ, 393pF
Driver	CGD15FB45P1

Fig. 8. Single module theoretical (solid line) and measured (dots) efficiencies for TCM and QSW-ZVS modes.

QSW-ZVS respectively. It should be noted that TCM works with the same input port current ripple and higher t_{d2}, hence, the reactive current is clearly higher than QSW-ZVS. However, the switching frequency has to be increased up to 66kHz for QSW-ZVS for the same current level as that with TCM.

B. Balanced technique

Once a single module has been tested, the IPOP modular converter under balanced technique is checked. The theoretical and experimental efficiencies are plotted in Fig. 10 for both TCM and QSW-ZVS modes. It should be remarked that

theoretical efficiencies have exactly the same shape of those efficiencies calculated for a single module, as it was expected. The experimental results follows the same tendency, therefore, the same conclusions obtained for a single module can be carried out here.

An example of the input port input current ripple is shown in Fig. 11 for QSW-ZVS mode when the IPOP converter operates at 4.8kW. As can be seen, the current ripple is around 5A, which is 0.3 times the total input current ripple measured for one module (as it was expected based on the theoretical analysis). As it was previously stated, both theoretical and measured efficiencies for QSW-ZVS is almost constant (98%) from 100% to 10% of maximum power. In the case of TCM, the efficiency is lower than 98% below 40% of full load.

C. Phase-shedding technique

The phase-shedding technique has been explored next. The theoretical and experimental efficiencies for this technique are plotted in Fig. 12 for both operational modes.

In comparison with balanced technique, the power range with high efficiency (above 98%) is wider. In the case of QSW-ZVS, the efficiency is kept almost constant down to 5% of full load.
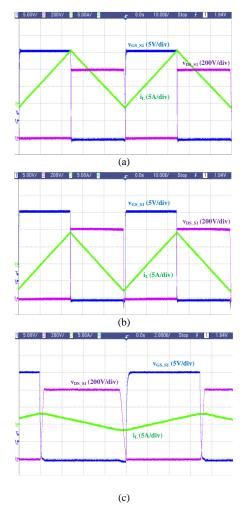

(a)

(b)

(c)

Fig. 9. Single module of IPOP converter main waveforms. (a) Full load for both QSW-ZVS and TCM, (b) light load for TCM and (c) light load for QSW-ZVS.
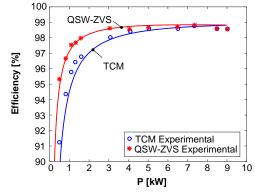

Fig. 10. Theoretical (solid) and measured (dots) efficiencies of a 3 module IPOP modular converter under balanced technique for TCM and QSW-ZVS operational modes.
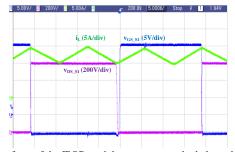

Fig. 11. Waveform of the IPOP modular converter under balanced technique QSW-ZVS at 4.8kW.
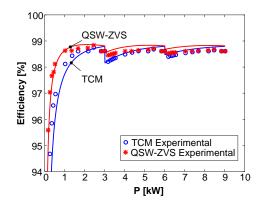

Fig. 12. Theoretical (solid) and measured (dots) efficiencies of a 3 module IPOP modular converter under phase-shedding control for TCM and QSW-ZVS operational modes.

In TCM, the improvement is even higher, extending the high efficiency from 40% to 10% of full load. It is finally noted that while the efficiency at full load is usually the most important one, there are applications for which the efficiency at light load can also be critical.

Averaged operating efficiencies, or weighted efficiencies, such as California Energy Commission (CEC) efficiency [34] or European (EURO) efficiency [35], [36], are examples of this efficiency conception different to the traditional one. TABLE II shows EURO and CEC efficiencies of the prototype for the four approaches. These weighted efficiencies confirm the advantage of QSW-ZVS over TCM and the advantage of phase-shedding control over balanced technique in terms of losses.

TABLE II.
EURO AND CEC EFFICIENCIES.

Option	EURO efficiency	CEC efficiency
TCM-Balanced technique	98.06%	98.46%
QSW-ZVS–Balanced technique	98.47%	98.62%
TCM-Phase-shedding	98.53%	98.55%
QSW-ZVS-Phase-shedding	98.63%	98.68%

VI. CONCLUSIONS

In this paper, the benefits of the use of SiC power MOSFETs are proposed and demonstrated in a high voltage synchronous boost converter. These devices can be switched at high frequency and they allow the use of QSW-ZVS operational mode in this converter to keep the efficiency high at light load (which is a key point in battery systems). Furthermore, a modular approach has been proposed to extend the advantage of the use of SiC power MOSFETs to higher power levels, wider power range with high efficiency and reduction of the input current ripple. These concepts have been explored by comparing this mode with TCM operational mode. And additional comparison of two different modular control techniques has been also carried out in terms of efficiency. Phase-shedding technique can be used to extend even more power range with high efficiency, obtaining almost plain efficiency from 100% to roughly 5% of full load (using QSW-ZVS), whereas balanced technique can be used if current ripple is more critical in the design.

REFERENCES

[1] Ronan, E.R.; Sudhoff, S.D.; Glover, S.F.; Galloway, D.L., "A power electronic-based distribution transformer," in Power Delivery, IEEE Transactions on , vol.17, no.2, pp.537-543, Apr 2002

[2] van der Merwe, J.W.; du T. Mouton, H.; , "The solid-state transformer concept: A new era in power distribution," AFRICON, 2009. AFRICON '09. , vol., no., pp.1-6, 23-25 Sept. 2009

[3] Jih-Sheng Lai; Maitra, A.; Mansoor, A.; Goodman, F.; , "Multilevel intelligent universal transformer for medium voltage applications," Industry Applications Conference, 2005. Fourtieth IAS Annual Meeting. Conference Record of the 2005 , vol.3, no., pp. 1893- 1899 Vol. 3, 2-6 Oct. 2005

[4] Xu She; Huang, A., "Solid state transformer in the future smart electrical system," in Power and Energy Society General Meeting (PES), 2013 IEEE , vol., no., pp.1-5, 21-25 July 2013

[5] J. Kolar and G. Ortiz, "Solid-state-transformers: key components of future traction and smart grid systems," in Proc. Of the International Power Electronics Conference (IPEC), Hiroshima, Japan, 2014

[6] Falcones, S.; Xiaolin Mao; Ayyanar, R., "Topology comparison for Solid State Transformer implementation," Power and Energy Society General Meeting, 2010 IEEE , vol., no., pp.1,8, 25-29 July 2010

[7] Zhao, T.; Wang, G.; Bhattacharya, S.; Huang, A. Q., "Voltage and Power Balance Control for a Cascaded H-Bridge Converter-Based Solid-State Transformer," Power Electronics, IEEE Transactions on , vol.28, no.4, pp.1523,1532, April 2013

[8] Xu She; Lukic, S.; Huang, A.Q.; Bhattacharya, S.; Baran, M.; , "Performance evaluation of solid state transformer based microgrid in FREEDM systems," Applied Power Electronics Conference and Exposition (APEC), 2011 Twenty-Sixth Annual IEEE , vol., no., pp.182-188, 6-11 March 2011

[9] Shojaei, A.; Joos, G., "A topology for three-stage Solid State Transformer," in Power and Energy Society General Meeting (PES), 2013 IEEE , vol., no., pp.1-5, 21-25 July 2013

[10] Briz, F.; Lopez, M.; Rodriguez, A.; Zapico, A.; Arias, M.; Diaz- Reigosa, D., "MMC based SST," in Industrial Informatics (INDIN), 2015 IEEE 13th International Conference on , vol., no., pp.1591-1598, 22-24 July 2015

[11] A. Lesnicar, and R. Marquardt, "An Innovative Modular Multilevel Converter Topology Suitable for a Wide Power Range", IEEE PowerTech Conference. Junio 23-26, 2003.

[12] Peftitsis, D.; Tolstoy, G.; Antonopoulos, A.; Rabkowski, J.; Lim, Jang-Kwon; Bakowski, M.; Angquist, L.; Nee, H-P, "High-power modular multilevel converters with SiC JFETs", Energy Conversion Congress and Exposition (ECCE), p. 2148-155, 12-16 Sept. 2010.

[13] J. Rodriguez, J.-S. Lai, and F. Z. Peng, "Multilevel inverters: A survey of topologies, controls, and applications" IEEE Trans. Ind. Electron., vol. 49, n. 4, p. 724-738. Ago. 2002.

[14] Rohner, S.; Bernet, S.; Hiller, M.; Sommer, R.; "Analysis and Simulation of a 6 kV, 6 MVA Modular Multilevel Converter", IEEE Industrial Electronics Conference (IECON). p. 225-230, 3-5 Nov. 2009.

[15] K. Young, C. Wang, L. Y. Wang and K. Strunz, "Chapter 2 – Electric Vehicle Battery Technologies," in Electric Vehicle Integration into Modern Power Networks, New York, Springer New York, 2013, pp. 15-56.

[16] José Millán; Philippe Godignon; Xavier Perpiñà; Amador Pérez-Tomás; José Rebollo, "A survey of wide bandgap power semiconductor devices", in Power Electronics, IEEE Transactions on, vol.29, no.5, May 2014.

[17] S. De Breucker, K. Engelen, R. D'hulst and J. Driesen, "Impact of current ripple on Li-ion battery ageing," 2013 World Electric Vehicle Symposium and Exhibition (EVS27), Barcelona, 2013, pp. 1-9.

[18] Vasiladiotis, M.; Rufer, A., "Analysis and Control of Modular Multilevel Converters With Integrated Battery Energy Storage," Power Electron., IEEE Trans. on , vol.30, no.1, pp.163,175, Jan. 2015

[19] M. A. Perez, D. Arancibia, S. Kouro and J. Rodriguez, "Modular multilevel converter with integrated storage for solar photovoltaic applications," Industrial Electronics Society, IECON 2013 - 39th Annual Conference of the IEEE, Vienna, 2013, pp. 6993-6998.

[20] R. Abhinav and N. M. Pindoriya, "Grid integration of wind turbine and battery energy storage system: Review and key challenges," 2016 IEEE 6th International Conference on Power Systems (ICPS), New Delhi, 2016, pp. 1-6.

[21] A. F. Burke, "Batteries and Ultracapacitors for Electric, Hybrid, and Fuel Cell Vehicles," Proceedings of the IEEE , vol. 95, no. 4, pp. 806-820 , April 2007.

[22] J. Miller, "Energy storage system technology challenges facing strong hybrid, plug-in and battery electric vehicles," Vehicle Power and Propulsion Conference, 2009. VPPC '09. IEEE , pp. 4-10, Sept. 2009.

[23] Yang, L.; Zhang, Y.; Lee, C.Q., "A family of constant-switching-frequency quasi-square-wave converters," Electrical and Computer Engineering, 1993. Canadian Conference on, vol., no., pp.309,312 vol.1, 14-17 Sep 1993.

[24] Yang, L.; Zhang, Y.F.; Lee, C.Q., "Analysis of the boost constant-frequency quasi-square-wave converters," Circuits and Systems, 1994., Proceedings of the 37th Midwest Symposium on, vol.2, no., pp.1172,1175 vol.2, 3-5 Aug 1994.

[25] Maksimovic, D., "Design of the zero-voltage-switching quasi-square-wave resonant switch," Power Electronics Specialists Conference, 1993. PESC '93 Record., 24th Annual IEEE, vol., no., pp.323,329, 20-24 Jun 1993.

[26] C. Marxgut, J. Biela and J. W. Kolar, "Interleaved Triangular Current Mode (TCM) resonant transition, single phase PFC rectifier with high efficiency and high power density,"Power Electronics Conference (IPEC), 2010 International, Sapporo, 2010, pp. 1725-1732.

[27] Vorperian, V., "Quasi-square-wave converters: topologies and analysis," Power Electronics, IEEE Transactions on , vol.3, no.2, pp.183,191, Apr 1988.

[28] Andreassen, Pal; Undeland, T.M., "Digital Control Techniques for Current Mode Control of Interleaved Quasi Square Wave Converter," Power Electronics Specialists Conference, 2005. PESC '05. IEEE 36th, vol., no., pp.910,914, 16-16 June 2005.

[29] Costa, J.M.F.D.; Silva, M.M., "Small-signal models and dynamic performance of quasi-square-wave ZVS converters with voltage-mode and current-mode control," Circuits and Systems, 1995., Proceedings., Proceedings of the 38th Midwest Symposium on, vol.2, no., pp.1183,1188 vol.2, 13-16 Aug 1995.

[30] Knecht, O.; Bortis, D.; Kolar, J.W., "Comparative Evaluation of a Triangular Current Mode (TCM) and Clamp-Switch TCM DC-DC Boost Converters," Energy Conversion Congress and Exposition (ECCE 2016, IEEE), vol., no., pp., 18-22 September 2016.

[31] S. Zhang, "Analysis and minimization of the input current ripple of Interleaved Boost Converter," 2012 Twenty-Seventh Annual IEEE Applied Power Electronics Conference and Exposition (APEC), Orlando, FL, 2012, pp. 852-856.

[32] A. Vazquez, A. Rodriguez, D. G. Lamar and M. M. Hernando, "Master-slave technique for improving the efficiency of interleaved synchronous boost converters," 2014 IEEE 15th Workshop on Control and Modeling for Power Electronics (COMPEL), Santander, 2014, pp. 1-9.

[33] Jen-Ta Su; Chih-Wen Liu, "A Novel Phase-Shedding Control Scheme for Improved Light Load Efficiency of Multiphase Interleaved DC–DC Converters," Power Electronics, IEEE Transactions on, vol.28, no.10, pp.4742,4752, Oct. 2013.

[34] C. W. C. E. C. B. Brooks, "Guideline for the use of the Performance Test Protocol for Evaluating Inverters Used in Grid-Connected Photovoltaic Systems," 2005. [Online]: http://www.gosolarcalifornia.ca.gov/equipment/documents/Sandia_Guideline_2005.pdf. [Last accessed: Feb. 2017].

[35] EC 1275/2008 Regulation of 2005/32/EC, EcoDesign. European Parliament. December 2008. [Online]: https://ec.europa.eu/growth/single-market/european-standards/harmonised-standards/ecodesign/standbyandoffmode_en [Last accessed: Feb. 2017].

[36] EC 278/2009 Regulation of 2005/32/EC, EcoDesign. European Parliament. April 2009. [Online]: https://ec.europa.eu/growth/single-market/european-standards/harmonised-standards/ecodesign/powersupplies_en. [Last accessed: Feb. 2017].

Aitor Vazquez (S'2010, M'2015) was born in Oviedo, Spain, in 1984. He received the M.Sc. degree in telecommunication engineering, in 2009, and the Ph.D. degree in electrical engineering in 2016, from the University of Oviedo, Gijon, Spain. Since 2010 he has been a researcher with the Power Supply System Group and an Assistant Professor with the Department of Electrical and Electronic Engineering at the University of Oviedo. His current research interests include modularization techniques applied to bidirectional dc–dc converters for HEV, battery management power supplies, DC distribution grids, power factor corrector ac–dc converters and energy recovery systems.

Alberto Rodriguez (S'2007, M'2014) was born in Oviedo, Spain, in 1981. He received the M.S. degree in telecommunication engineering in 2006 from the University of Oviedo, Gijón, Spain, and the Ph.D. degree in electrical engineering in the same university in 2013. Since 2006, he has been a researcher with the Power Supply System Group and an Assistant Professor with the Department of Electrical and Electronic Engineering at the University of Oviedo. His research interests are focused on multiple ports power supply systems, bidirectional DC-DC power converters and wide band gap semiconductors.

Maria R Rogina (S'2014) was born in Aviles, Spain, in 1990. She received the M.Sc. degree in telecommunication engineering from the University of Oviedo, Spain, in 2014, and she is currently pursuing the Ph.D. degree in the same university. Her research interests include switching-mode power supplies, dc-dc converter modelling and bidirectional DC-DC power converters.

Diego G. Lamar (M'2008) was born in Zaragoza, Spain, in 1974. He received the M.Sc. degree, and the Ph.D. degree in Electrical Engineering from the University of Oviedo, Spain, in 2003 and 2008, respectively. In 2003 and 2005 he became a Research Engineer and an Assistant Professor respectively at the University of Oviedo. Since September 2011, he has been an Associate Professor. His research interests are focused in switching-mode power supplies, converter modelling, and power-factor-correction converters.